PHYSICAL REVIEW B **76**, 121404(R) (2007)

Vibrations of nanoparticles: From nanospheres to fcc cuboctahedra

B. Stephanidis,[1] S. Adichtchev,[1] S. Etienne,[2,3] S. Migot,[3] E. Duval,[1] and A. Mermet[1]
[1]*Laboratoire de Physicochimie des Matériaux Luminescents, Université de Lyon, Université Lyon 1, CNRS, Domaine scientifique de la Doua, Bâtiment Kastler, 10 rue Ampère, Villeurbanne F-69622, France*
[2]*Ecole Européenne d'Ingénieurs en Génie des Matériaux, Nancy Université, 6 rue Bastien Lepage, 54010 Nancy Cedex, France*
[3]*Laboratoire de Physique des Matériaux, UMR CNRS 7556, Ecole des Mines, 54042, Nancy Cedex, France*
(Received 20 August 2007; published 27 September 2007)

Vibrational modes of gold nanoparticles grown in a silicate glass were studied through high-resolution low-frequency Raman scattering. The spectra evidence a clear splitting of the quadrupolar mode into two components, unseen in lower-resolution Raman experiments. This splitting turns out to be quantitatively consistent with the lifting of degeneracy expected as the nanoparticles evolve from nanospheres to faceted crystalline nanocrystals.

DOI: 10.1103/PhysRevB.76.121404 PACS number(s): 78.30.−j, 78.67.Bf, 63.22.+m

Vibrational energy in condensed matter is sustained by vibration modes characterized by a wavelength λ and an energy $E=h\nu$, where ν is the vibrational frequency. For any finite-size object, when the wavelength of the mode becomes comparable with the size of the object itself, the whole object is set into a coherent oscillating motion. These oscillation modes provide unique insight into subtle dynamical changes of the objects' shapes, from planets[1,2] to nanometer-size particles.[3,4] So far the experimental studies of nanoparticle vibration modes have focused on highly symmetrical objects like spheres (from nanometric metallic clusters[3–5] to submicrometer glass nanobeads[6–8]), essentially through inelastic light scattering. In this paper, we report detection of the vibration modes from crystalline nanopolyhedra and provide their physical interpretation.

Similarly to the eigenmodes of a fixed string, the fundamental oscillation frequency of a free sphere of diameter D is approximately given by[1]

$$\nu \approx \frac{v}{D}, \tag{1}$$

where v refers to an orientationally averaged speed of sound inside the sphere. Qualitatively, this relation has shown to account sufficiently well for the experimentally determined frequencies, although observed samples hardly ever consist of nanoparticles that are *freely* vibrating *perfect spheres*. While recent developments allowed one to account quantitatively for the more realistic case of nanoparticles confined in a host medium,[9,10] the often off-spherical morphology of the nanoparticles has scarcely been considered.[11] Regarding the growing interest in nonspherical nanoparticles like nanoprisms, nanorods, or polyhedral biological particles like viruses,[12–15] this aspect deserves a thorough examination.

Gold nanoparticles were grown in a multicomponent silicate glass with initial gold molar content of 0.06%. Four samples were differentiated through different times of annealing at 470 °C, slightly above the glass transition temperature. Upon annealing, the Au-doped glasses progressively develop a ruby shade, which is typical of gold clusters. Figure 1 shows the absorption spectra from a series of four samples annealed around the glass transition temperature over times ranging between 8 and 68 h. These spectra show the well-known surface plasmon resonance (SPR) peak of the metallic nanoparticles, shifting from 527 nm to 532 nm as the annealing time is increased. Quite remarkably, the SPR experimental linewidths found for these systems are as low as, if not lower than, those measured from unique gold nanoparticles of comparable sizes[16] (≃0.15 eV half width at half maximum). This is an indication that both the size and the shape distributions of the so-produced gold nanoparticle assemblies are relatively narrow, as supported by electron microscopy observations. In the following, the strong SPR is harnessed through resonant Raman scattering to probe the vibrational modes of the embedded gold nanoparticles.

Figure 2 shows the Stokes–anti-Stokes Raman spectra of the samples, recorded with a six-pass tandem Fabry-Pérot interferometer,[17] using the 532 nm line of a continuous yttrium aluminum garnet (YAG) laser, i.e., in resonance with the SPR, in backscattering geometry. The use of a spectroscopic device of a much higher resolving power than those currently used in Raman spectroscopy allows us to evidence substructures in what would have otherwise appeared as a two-component spectrum[18] (Fig. 2 inset). These two "sphere" components have long been identified as two of the possible spheroidal modes of a nano sphere, namely, the qua-

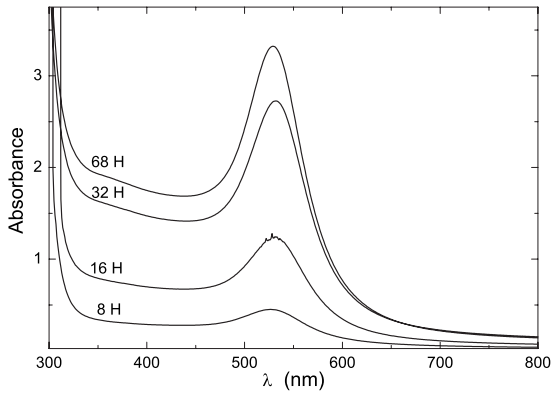

FIG. 1. Absorption spectra of glasses containing Au nanocrystals for different annealing times.

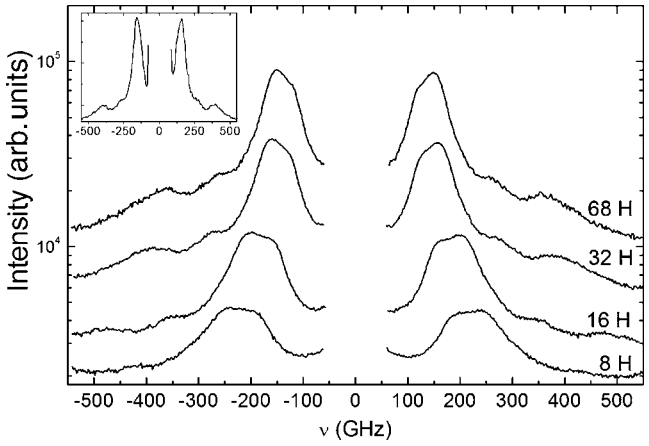

FIG. 2. Raman spectra (in log-linear scale) of Au nanocrystals embedded in glasses annealed over different times, as derived from measurements with a six-pass tandem Fabry-Pérot interferometer. The inset shows the spectrum of the sample annealed for 32 h, recorded with a lower-resolution monochromator (Ref. 18)

drupolar mode and the spherical mode (in the present experiments, only the fundamental harmonics of both modes are detected). While the former, of lower frequency, shows up as a depolarized intense band, the latter appears as a polarized band with weaker intensity due to less efficient coupling with the dipolar plasmon excitations.[19] From the comparison between a low-resolution spectrum (Fig. 2 inset) and its high-resolution counterpart (curve of the sample annealed for 32 h in Fig. 2), one can roughly recognize the two sphere features, yet the quadrupolar line shows pronounced substructures and an additional small bump is observed in its high-energy foot. These new features are observed to be depolarized, like the quadrupolar mode of a sphere.

The first explanations that can be thought of to justify the subcomponents in the low-frequency Raman spectra from an assembly of nanoparticles are a multimodal size distribution and/or nonspherically shaped nanoparticles (like ellipsoids). These hypotheses, however, are discarded as they conflict the remarkable narrowness of the single SPR peak. Interestingly, the transmission electron microscopy (TEM) pictures of some samples randomly picked from the series clearly evidence a faceting of the Au nanoparticles [Fig. 3(a)]. As expected from the face centered cubic (fcc) structure of Au, the TEM observations are consistent with two-dimensional projections of cuboctahedra or truncated cuboctahedra [Fig. 3(b)]. We show hereafter that the symmetry group change as the nanoparticle shape changes from a sphere [symmetry group O(3))] to a cuboctahedron (symmetry group O_h) is responsible for the splitting of the quadrupolar vibrational mode observed in Fig. 2; this interpretation explains the experimental data in a surprisingly successful way.

The oscillating modes of a sphere are characterized by an orbital quantum number ℓ, which is 0 for the spherical mode and 2 for the quadrupolar mode. These two modes were shown to be the only ones to be Raman active,[21] from low-resolution observations like that of Fig. 2 (inset). The vibration frequencies of these modes are given by

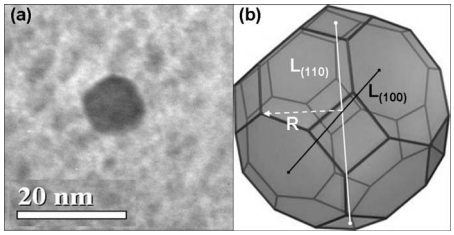

FIG. 3. (a) TEM picture (Ref. 20) of a Au nanoparticle embedded in the sample annealed for 68 h. (b) Representation of a truncated cuboctahedron, where R is the radius of the circumscribed sphere; $L_{(100)}$ and $L_{(110)}$ are the separations between opposite (100) octogonal and (110) square faces of the truncated cuboctahedron, respectively.

$$\nu_{sph} \simeq S_{sph}\frac{\langle v_L\rangle}{D} \quad \text{and} \quad \nu_{quad} \simeq S_{quad}\frac{\langle v_T\rangle}{D}, \tag{2}$$

where $\langle v_L\rangle$ and $\langle v_T\rangle$ are, respectively, the orientationally averaged longitudinal and transverse speeds of sound inside the nanoparticle. For a given shape, the values of S_{sph} and S_{quad} depend on the ratio $\langle v_T\rangle/\langle v_L\rangle$. In the case of spheres, using the values of bulk gold [$\langle v_L\rangle$=3319 m/s and $\langle v_T\rangle$ =1236 m/s, (Ref. 22)] S_{sph}=0.94 and S_{quad}=0.845. Taking for ν_{quad} the position of the maximum intensity in the lower-frequency intense band (quadrupolar mode), one obtains from Eq. (2) diameters increasing from 4 to 7 nm with increasing annealing time.

If one now considers that the nanoparticles are not exactly isotropic elastic spheres but rather fcc *cuboctahedra* (or *truncated cuboctahedra*), the scattering condition by only the ℓ =0 and 2 modes of a sphere needs to be revised. Going from a spherical symmetry to the octahedral symmetry of a cuboctahedron, the fivefold degeneracy of the quadrupolar mode $(2\ell+1)$ is lifted into a twofold degenerate mode with symmetry E_g and a threefold degenerate mode with symmetry T_{2g}. Similarly, the nondegenerate spherical mode becomes an A_{1g} mode in octahedral symmetry. As vibrational modes of a faceted fcc nanocrystal, the E_g, T_{2g}, and A_{1g} modes are to be identified with the longitudinal and transverse elastic waves confined in the cubic nanocrystals.[23] To do so, one first observes that the elastic fcc structure of gold is strongly anistropic, as attested by its high Zener anisotropy ratio $2C_{44}/(C_{11}-C_{12})$=2.9 (C_{44}, C_{11}, and C_{12} are the usually defined elastic constants[23]). For such anisotropic structures, Saviot and Murray[24] recently pointed out that the ℓ=2 modes of spheres have a marked *transverse* character, while the ℓ =0 modes are strongly *longitudinal*. Among the possible transverse elastic waves confined in a cubic structure, essentially those propagating along the [100] directions with the classically defined transverse speed of sound $v_{T_{2g}}=\sqrt{C_{44}/\rho}$ (where ρ is the mass density of gold) transform as in the T_{2g} representation, regarding the O_h point group of a cuboctahedron, with corresponding strains $(1/\sqrt{2})(\epsilon_{yz}+\epsilon_{zy})$, $(1/\sqrt{2})$ $\times(\epsilon_{zx}+\epsilon_{xz})$, and $(1/\sqrt{2})(\epsilon_{xy}+\epsilon_{yx})$. In the same way, the E_g representation $((1/\sqrt{2})(\epsilon_{xx}-\epsilon_{yy})$ and $(1/\sqrt{6})(2\epsilon_{zz}-\epsilon_{xx}-\epsilon_{yy}))$ is essentially compatible with the transverse modes propagat-

ing along the [110] directions with the speed of sound $v_{E_g} = \sqrt{(1/2)(C_{11}-C_{12})/\rho}$. As for the A_{1g} modes, they identify with the longitudinal modes propagating along the [100] directions with the usually defined longitudinal speed sound given by $v_L = \sqrt{C_{11}/\rho}$. Note that the plane waves propagating along the [100] and [110] directions of an infinite crystal turn, in the case of a nanocrystal, into *stationary* waves because of the confinement between the respectively opposite (100) and (110) faces of the faceted nanoparticle. Assuming one gold nanocrystal as a truncated cuboctahedron inscribed within a cube of edge a, the confining distance for the T_{2g} modes is the separation between opposite (100) faces of the truncated cuboctahedron [Fig. 3(b)], i.e., $L_{(100)}=a$. The confining distance for the E_g modes is $L_{(110)}=1.293a$.

It comes out from this analysis that for faceted nanocrystals only three types of fundamental modes (T_{2g}, E_g, and A_{1g}) should be observed. Figure 2 evidences four components: two overlapping low-energy components with an additional small one lying in their high-energy foot and one lying at higher energy. As shown below, the most likely explanation is that the high-resolution spectra still feature the dominating signal from nanospheres (with the $\ell=0$ and the 2 lines), in addition to those of the T_{2g} and E_g modes inherent to coexisting faceted nanocrystals. As for the A_{1g} mode, due to its weak intensity and close vicinity to the spherical mode, its existence could not be established.

Following Eq. (1), the frequencies of the T_{2g} and E_g modes associated with a cuboctahedral nanocrystal are given by $\nu_{T_{2g}} \simeq v_{T_{2g}}/L_{(100)}$ and $\nu_{E_g} \simeq v_{E_g}/L_{(110)}$. If the nanocrystal's detailed morphology is closer to a sphere than to a cuboctahedron, then its quadrupolar frequency is given by Eq. (2), using as mean diameter $\bar{D}$ the average value between those of the circumscribed and inscribed spheres of the truncated cuboctahedron, i.e., $\bar{D} \simeq 1.2a$. Consequently, the frequency ratio between the E_g component of a faceted nanocrystal and the quadrupolar mode of a nanosphere is given by

$$\frac{\nu_{E_g}}{\nu_{quad}} \simeq \frac{v_{E_g}}{L_{(110)}} \left(S_{quad} \frac{\langle v_T \rangle}{\bar{D}} \right)^{-1}, \tag{3}$$

and the frequency ratio between the T_{2g} component of a faceted nanocrystal and the quadrupolar frequency of a nanosphere is

$$\frac{\nu_{T_{2g}}}{\nu_{quad}} \simeq \frac{v_{T_{2g}}}{L_{(100)}} \left(S_{quad} \frac{\langle v_T \rangle}{\bar{D}} \right)^{-1}. \tag{4}$$

Substituting the values $v_{E_g}=867$ m s^{-1} and $v_T=1483$ m s^{-1}, as derived from the elastic constants of bulk gold,[22] the expected frequency ratios are

$$\frac{\nu_{E_g}}{\nu_{quad}} \simeq 0.77 \quad \text{and} \quad \frac{\nu_{T_{2g}}}{\nu_{quad}} \simeq 1.70. \tag{5}$$

Similarly, the frequency ratio between the quadrupolar mode and the spherical mode, for a given diameter $\bar{D}$ is

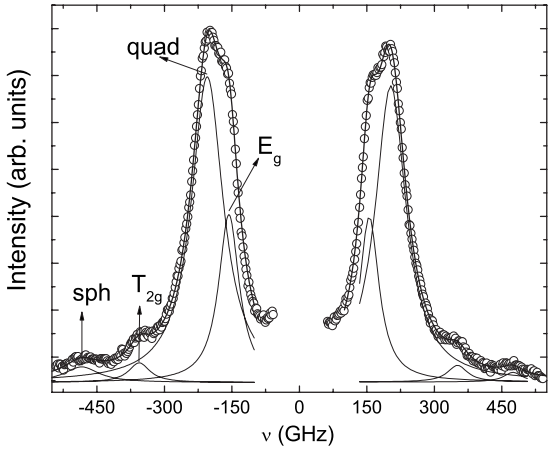

FIG. 4. Four Lorentzian fits (lines) of the high-resolution spectrum (symbols) of the sample annealed during 68 h. The four subcomponents are labeled according to the text.

$$\frac{\nu_{sph}}{\nu_{quad}} = \left(S_{sph} \frac{\langle v_L \rangle}{\bar{D}} \right) \left(S_{quad} \frac{\langle v_T \rangle}{\bar{D}} \right)^{-1} \simeq 2.99. \tag{6}$$

Figure 5 compares the above expected frequency ratios with the experimental values derived from four Lorentzian fits of the Raman data (Fig. 4). The very good agreement between experimental and theoretical values of the frequency ratios, whatever the sizes of the nanocrystals, validates the proposed interpretation. The discrepancy observed between the theoretical and experimental values of ν_{sph}/ν_{quad} is entirely ascribable to the case of *freely* vibrating nanospheres: taking into account the influence of the embedding medium[9] lowers the ratio from 2.99 to 2.48, therefore perfectly matching that found experimentally. The presence of the embedding medium is not relevant for the two other ratios as they concern modes of similar origin (i.e., transverse).

As a conclusion, we have shown that low-frequency vibrational modes of nanoparticles can be differentiated as the elastic nanoparticles evolve from isotropic spheres to faceted crystalline polyhedra. Upon lowering the symmetry, the de-

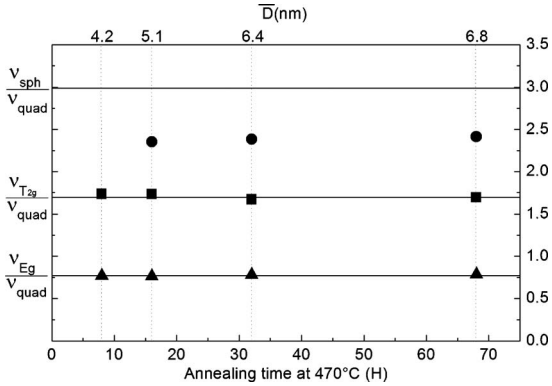

FIG. 5. Comparison of the theoretical (horizontal lines) and experimental (symbols) frequency ratios of the spherical $\ell=0$, T_{2g}, and E_g modes to the quadrupolar $\ell=2$ mode. The top scale indicates the mean diameter of the nanoparticles, as derived from ν_{quad} [Eq. (2)].

generacies of the modes are lifted or partially lifted, leading to a splitting of the nanosphere single components. The presently reported case of gold cuboctahedra, nucleated in a silicate glass with a remarkably narrow size distribution, has allowed us to quantitatively verify the expected frequency splittings of the nanosphere quadrupolar mode. This has been possible thanks to the use of a very high-resolution spectrometer. It is noteworthy that the relative intensities of the split components do not scale with the degeneracy levels. As a result of a resonant Raman process, these intensities are expected to be controlled by the coupling strength with the dipolar plasmon excitation, which differs from one mode to another. This situation will be clarified by theoretical investigations.

[1] H. Lamb, Proc. London Math. Soc. **13**, 189 (1882).
[2] L. T. Chadderton, F. G. Krajenbrink, R. Katz, and A. Poveda, Nature (London) **223**, 259 (1969).
[3] E. Duval, A. Boukenter, and B. Champagnon, Phys. Rev. Lett. **56**, 2052 (1986).
[4] A. Courty, A. Mermet, P. A. Albouy, E. Duval, and M. P. Pileni, Nat. Mater. **4**, 395 (2005).
[5] B. Palpant, H. Portalès, L. Saviot, J. Lermé, B. Prével, M. Pellarin, E. Duval, A. Perez, and M. Broyer, Phys. Rev. B **60**, 17107 (1999).
[6] J. Liu, L. Ye, D. A. Weitz, and P. Sheng, Phys. Rev. Lett. **65**, 2602 (1990).
[7] R. S. Penciu, M. Kafesaki, G. Fytas, E. N. Economou, A. Steffen, W. Hollingsworth, and W. B. Russel, Europhys. Lett. **58**, 699 (2002).
[8] M. H. Kuok, H. S. Lim, S. C. Ng, N. N. Liu, and Z. K. Wang, Phys. Rev. Lett. **90**, 255502 (2003).
[9] D. B. Murray and L. Saviot, Phys. Rev. B **69**, 094305 (2004).
[10] L. Saviot, D. B. Murray, and M. C. Marco de Lucas, Phys. Rev. B **69**, 113402 (2004).
[11] J. Margueritat, J. Gonzalo, C. Afonso, A. Mlayah, D. Murray, and L. Saviot, Nano Lett. **6**, 2037 (2006).
[12] P. de Gennes and M. Papoular, *Polarisation Matière et Rayonnement* (PUF Société Française de Physique, Paris, 1969), pp. 243–258.
[13] L. H. Ford, Phys. Rev. E **67**, 051924 (2003).
[14] L. Saviot, D. B. Murray, A. Mermet, and E. Duval, Phys. Rev. E **69**, 023901 (2004).
[15] B. Stephanidis, S. Adichtchev, P. Gouet, A. McPherson, and A. Mermet, Biophys. J. **93**, 1354 (2007).
[16] S. Berciaud, L. Cognet, P. Tamarat, and B. Lounis, Nano Lett. **5**, 515 (2005).
[17] S. M. Lindsay, M. W. Anderson, and J. R. Sandercock, Rev. Sci. Instrum. **52**, 1478 (1981).
[18] The lower-resolution spectrum was obtained with a quintuple monochromator working with entrance and exit slits of 120 μm. The same excitation wavelength was used, as well as the same power (150 mW). The scattered light was collected off the specular reflection, at 90° from the incident light.
[19] H. Portalès, L. Saviot, E. Duval, M. Fujii, S. Hayashi, N. Del Fatti, and F. Vallée, J. Chem. Phys. **115**, 3444 (2001).
[20] The TEM observations were made with a Philips CM 200.
[21] E. Duval, Phys. Rev. B **46**, 5795 (1992).
[22] These values are derived from the elastic constants of Au, as retrieved from *The Elastic Constants of Crystals and Other Anisotropic Materials*, Landolt-Börstein Tables (Springer-Verlag, Berlin, 1984), pp. 1–154: $C_{11}=191$ GPa, $C_{12}=162$ GPa, $C_{44}=42$, 4 GPa and $\rho=19283$ kg.m^{-3}.
[23] C. Kittel, *Introduction to Solid State Physics*, 7th ed. (Wiley, New York, 1996), pp. 88–91.
[24] L. Saviot and D. B. Murray, Phys. Rev. B **72**, 205433 (2005).